

RSC Advances



This is an *Accepted Manuscript*, which has been through the Royal Society of Chemistry peer review process and has been accepted for publication.

Accepted Manuscripts are published online shortly after acceptance, before technical editing, formatting and proof reading. Using this free service, authors can make their results available to the community, in citable form, before we publish the edited article. This *Accepted Manuscript* will be replaced by the edited, formatted and paginated article as soon as this is available.

You can find more information about *Accepted Manuscripts* in the [Information for Authors](#).

Please note that technical editing may introduce minor changes to the text and/or graphics, which may alter content. The journal's standard [Terms & Conditions](#) and the [Ethical guidelines](#) still apply. In no event shall the Royal Society of Chemistry be held responsible for any errors or omissions in this *Accepted Manuscript* or any consequences arising from the use of any information it contains.

Bio-functionalized nanofibrous membranes as a hybrid platform for selective antibody recognition and capturing

*Jing Zhu and Gang Sun**

Fiber and Polymer Science, University of California, Davis, CA 95616, United States

Abstract

Poly (vinyl alcohol-*co*-ethylene) (PVA-*co*-PE) is attractive for a variety of bio-applications due to its intrinsic hydrophilicity and ease of functionalization. The successful preparation of PVA-*co*-PE nanofibrous membranes and its applications as an ideal matrix for enzyme immobilization and dye/metal affinity purification have been reported. In this study, we specifically focused on versatile surface chemistries to activate PVA-*co*-PE nanofibers and their subsequent protein ligand couplings for antibody recognition and capturing, where surface activation can afford the largest amount as well as the highest activity of immobilized protein ligand. Protein A/G and immunoglobulin G (IgG) were applied here as a model pair of affinity ligand and antibody target. Disuccinimidyl carbonate (DSC) was found to offer the highest amount of immobilized affinity ligands. However, its high reactivity toward hydroxyl and amine groups from protein molecules may trigger multi-binding effect of immobilized ligands and subsequently limit the conformation changes of the ligands, eventually leading to a low ligand activity. Among all of the tested agents, Glutaraldehyde (GA) was observed to provide the highest antibody binding capacity as a synergetic result of the high ligand activity and the desired amount of attached ligands. Its higher ligand activity can be ascribed to the potential spacer effect of the oligomeric units formed by GA molecules. The excellent selectivity and efficient capturing ability for target antibody, the desired stability and reliable reusability of proteinA/G attached GA pre-activated PVA-*co*-PE nanofibrous membranes were demonstrated through IgG static binding capacity test and

SDS-PAGE analysis. These exciting results indicate the great potential of the bio-functionalized nanofibrous membranes as a hybrid platform for selective antibody recognition and purification.

Keywords: nanofibrous membrane, protein A/G, immunoglobulin G, selective antibody recognition and purification

Corresponding author: Gang Sun, Tel: (530)752-0840; Fax: (530)752-7584; Email:

gysun@ucdavis.edu

Introduction

Over the last two decades, there has been an exponential growth of the market for antibody products due to the broad applications of antibodies in many important areas such as bio-therapeutics, disease diagnosis and immuno-affinity chromatography.¹⁻³ As a result, versatile technologies like precipitation, ultrafiltration and bio-chromatography have been exploited for antibody purification and polishing in order to facilitate the downstream processes.⁴ Among these methods, bio-chromatography is most extensively employed owing to the highly bio-specific and reversible interactions between affinity ligands and target antibodies. In general, the affinity interactions include ion exchange (IEX), hydrophobic interaction (HIC), immobilized metal affinity chromatography (IMAC), and bio-recognition with protein ligands, among which protein ligand (such as protein A, G, or A/G) based affinity chromatography exhibits the best purification performance in terms of the highest selectivity and binding capacity toward immunoglobulin G (IgG).⁵⁻⁷ The protein A, a single polypeptide chain, consists of four high-affinity binding sites capable of specifically reacting with the Fc region from IgG. Similar to the protein A from cell wall proteins, the protein G contains two IgG-binding domains as well as albumin binding sites. Recently, an engineered gene fusion protein ligand, protein A/G, has been developed by combining four Fc-binding domains from the protein A with two domains from the protein G.^{8,9} In comparison to the protein A and the protein G, the advantages of this protein ligand includes an even stronger affinity effect, the absence of binding sites for undesired biomolecules, and enhanced stability in a broader range of pH values.¹⁰

Acting as a support platform for affinity ligands, solid matrix possesses the nature of hydrophilicity, spacer length, surface charge and function density, which is crucial for final performance of antibody purification. Micro-sized beads possess high surface area due to their enormous interior pores, resulting to a high surface density of immobilized ligands for efficient antibody capture.¹¹ So far,

chromatography based on bead-packed columns is the most commonly used. Despite the advantages mentioned above, the limitations, such as high pressure drop, slow intra-particle diffusion of biomolecules and difficulty in large column packing, become the bottleneck for the large-scaled application of this technology.¹² Originally designed to circumvent the above practical issues, affinity membrane is an attractive and competent tool for antibody purification. However, conventional membrane matrices usually have low surface area, leading to a low amount of immobilized ligands and accessing difficulty to these ligands. Therefore, a variety of efforts has been devoted to develop new membrane systems that can achieve high protein purification performance.^{13, 14} Nanofibrous membranes can serve as an ideal candidate for this purpose. The open porous nonwoven structural feature of the nanofibrous membranes can provide a desired fast mass transfer rate through the system. In addition, the superior mechanical and chemical stabilities of properly selected polymers enable the prepared nanofibrous membrane to stand for extreme conditions used for purification processes. Moreover, their high surface area to volume ratio and ability for easy functionalization make the versatile ligand immobilization more approachable with a high loading capacity. Though several synthetic and natural polymeric nanofibrous membranes for selective protein adsorptions have been prepared¹⁵⁻²⁵, the innovation of nanofibrous membranes with enhanced antibody recognition and capturing performance is still in the infancy with respect to the traditional column based method.

Our previous studies demonstrated that hydrophilic PVA-*co*-PE nanofibrous membranes possess high density of reactive sites on surfaces and the good stability against harsh acidic/basic conditions, which could be beneficial for protein immobilizations. More importantly, its hydrophilic nature enables ultralow nonspecific protein adsorption, which is a critical characteristic for an ideal affinity membrane.²⁶⁻²⁸ To further explore the feasibility of applying the unique nanofibrous membranes in antibody purification, versatile chemical modifications on the membrane surfaces were investigated

through the study of the reaction kinetics of a couple of activation agents. The ease of coupling and non-specific binding to the protein A/G ligand, the static binding capacity to IgG, and practical IgG separation and purification from biomass mixtures by using the prepared membrane systems were the factors to evaluate the prepare bio-functionalized PVA-*co*-PE nanofibrous membranes in antibody purifications.

Experiment

1. Materials

Poly (vinyl alcohol-*co*-ethylene) (PVA-*co*-PE, ethylene content 27%), bovine serum albumin (BSA, 98% agarose gel electrophoresis, 66 kDa), FITC-IgG from human serum, human IgG (Technical Grade, Sigma), epibromohydrin (EP), nitrophenyl chloroformate (NP), cyanuric chloride (CC), carbonyldiimidazol (CDI), glutaraldehyde (GA), disuccinimidyl carbonate (DSC) and 1,4-butanediol diglycidyl ether (BDGE). 4-(dimethylamino) pyridine were purchased from Sigma–Aldrich (Milwaukee, WI, USA). Protein A/G was purchased from Thermo (Rockford, IL, USA). Cellulose acetate butyrate (CAB, butyryl content 44–48 wt %), triethylamine, acetone, dioxane and DMF were purchased from Acros Organics (Pittsburg, PA, USA). Buffers were prepared using analytical grade chemicals, and distilled water was purified via a Millipore Milli-Q plus water purification system.

2. Fabrication of nanofibrous membranes

The preparation of PVA-*co*-PE nanofibers was conducted based a previously reported procedure.²⁹⁻³¹ Typically, PVA-*co*-PE is mixed with CAB in a blend ratio of CAB/PVA-*co*-PE at 80/20, which is gravimetrically fed into a Leistritz co-rotating twin-screw (18 mm) extruder (Model MIC 18/GL 30D, Nurnberg, Germany) at a feed rate of 12 g/min. The immiscible polymer blends are

extruded into composite fibers through a two strand (2 mm in diameter) rod die, hot-drawn by a take-up device with a drawing ratio of 25 (the area of cross-section of the die to that of the extrudates) and air cooled to room temperature. Then, CAB/PVA-*co*-PE composite fibers are Soxhlet extracted by acetone to remove CAB matrix. To fabricate PVA-*co*-PE nanofibrous membrane, the prepared nanofibers are well dispersed and air-spray deposited onto a polyester monofilament fabric as a releasing surface.

3. Surface activation of nanofibrous membranes

A. *Epibromohydrin (EP)*. 20 mg original membrane was immersed into a mixed solution containing 2 mL alkaline aqueous solution (0.5M NaOH) and 2 mL EP overnight, followed by extensive washing with deionized water and drying in vacuum.

B. *1,4-Butanediol diglycidyl ether (BDGE)*. 2 mL BDGE was mixed with 2 mL alkaline aqueous solution (0.5M NaOH) with small amount of NaBH₄. 20 mg original membrane was added into the mixture overnight. The resulted membrane was extensively washed with deionized water and dried in vacuum.

C. *Oxalyl Chloride (OA)*. 20 mg original membrane was immersed into 4 mL dry dioxane with previously dissolved triethylamine (3 mmol) for 30 min. And then 2 mmol OA was added into the solution for 4 h. The resulted membrane was washed with dioxane and acetone, and dried in vacuum.

D. *Nitrophenyl Chloroformate (NP)*. 20 mg original membrane was immersed in 4 mL dry dioxane with previously dissolved NP (2 mmol) and triethylamine (3 mmol) for 4 h. The resulted membrane was washed with dioxane and acetone, and dried in vacuum.

E. *Cyanuric Chloride (CC)*. 20 mg original membrane was first activated in alkaline aqueous solution (3 M) for 1 h. After draining the excess alkaline solution, 4 mL dioxane with previously

dissolved 2 mmol CC was added for 4 h. The resulted membrane was washed with dioxane, deionized water and acetone, and dried in vacuum.

F. *Carbonyldiimidazol (CDI)*. 20 mg original membrane was immersed into 4 mL dry DMF with previously dissolved 2 mmol CDI. After 6 h reaction, the resulted membrane was washed with DMF and acetone, and dried in vacuum.

G. *Glutaraldehyde (GA)*. 20 mg original membrane was immersed in 20% GA solution with pH at 3 overnight. The resulted membrane was extensively washed with deionized water and dried in vacuum.

H. *Disuccinimidyl carbonate (DSC)*. 2 mmol DSC and 2 mmol DMAP were dissolved in 4 mL dry dioxane, in which 20 mg original membrane was added. After running overnight, the resulted membrane was washed with dioxane and acetone, and dried in vacuum.

4. Immobilization of BSA and protein A/G on activated nanofibrous membranes

BSA immobilization was conducted by immersing 20 mg membrane sample in a prepared 0.1M phosphate buffer (pH 7) with BSA concentration at 2 mg/mL for different incubation times. After the incubation, resulted membrane sample was washed with plenty of phosphate buffer carrying 1% Tween 20 until no BSA can be detected in washing solution. The amount of immobilized BSA on the membrane surfaces was calculated by measuring the difference between the initial and final BSA concentrations in adsorption media, and the BSA concentration was determined by a bicinchoninic acid assay using a Pierce BCA Protein Assay Kit.³² Protein A/G immobilization was conducted by 20 mg membrane sample in prepared 0.1M phosphate buffer (pH 7) with protein A/G concentration at 2 mg/mL for overnight. After the incubation, resulted membrane sample was washed with plenty of phosphate buffer carrying 1% Tween 20 until no protein A/G can be detected in washing solution. The

amount of immobilized IgG on membrane surfaces was determined by using the same method for BSA described above.

5. Fluorescein isothiocyanate (FITC) labeled human IgG (FITC-IgG) adsorption

FITC-IgG solutions in various initial concentrations were prepared in diluted Pierce Protein A/G IgG Binding Buffers. 20mg protein A/G immobilized membrane or original PVA-co-PE membrane were immersed in above FITC-IgG solutions for 4hrs at room temperature. And then, these membranes were thoroughly washed with phosphate buffer until no FITC-IgG was found in the washing solutions. And these membranes were dried and stored in a vacuum before further testing. The fluorescent microscopy images of these -IgG adsorbed membranes were obtained by using a laser scanning confocal microscope of the Olympus America FV1000 system (Olympus/PA, USA).

6. Static IgG adsorption

Human IgG solutions in different initial concentrations were prepared in diluted Pierce Protein A/G IgG Binding Buffer. After immersing 20 mg protein A/G immobilized membrane in IgG solution for certain time, the membrane sample was thoroughly washed with the phosphate buffer to remove free IgG molecules. The IgG concentration in washing solutions was determined by measuring its UV absorbance at 280 nm based on previously established standard curve.³³ Original membrane was tested under the same procedure as controls. The IgG adsorption isotherm on the prepared affinity membranes was studied based on the following Langmuir equation (Equation 1),

$$\frac{1}{q} = \frac{K_d}{q_m \times C} + \frac{1}{q_m} \quad (1)$$

where q_m is the maximum adsorption capacity (mg/g), K_d is the dissociation constant of the system (mg/mL), q is the adsorbed IgG on nanofiber (mg/g) and C is the equilibrium IgG concentration (mg/mL).

7. IgG purification

A protein mixture was prepared by dissolving IgG (2 mg/mL) and BSA (0.5 mg/mL) in diluted Pierce Protein A/G IgG Binding Buffer. 20 mg protein A/G immobilized membrane was immersed into this mixture for 4 h and followed by washing with the phosphate buffer to remove free IgG and BSA molecules. And then, the IgG adsorbed membrane was added into 1 mL Pierce™ IgG Elution Buffer for 2 h, and the IgG concentration in eluted solution was determined by its UV absorbance mentioned before. In order to examine the reusability of the prepared membranes for IgG purification, the same membrane sample after first trial was collected and washed before applied to the fresh protein mixtures for repeated tests. The purity of the eluted IgG was examined via sodium dodecyl sulfate polyacrylamide gel electrophoresis (SDS-PAGE) with 12% polyacrylamide gels and Pierce unstained protein molecular weight marker (Thermo, Rockford, IL, USA). Coomassie blue staining protocol was employed to visualize the protein bands.

8. Instrument analysis

Morphologies of nanofibrous membranes were observed by using a scanning electron microscopy (SEM) (XL 30-SFEG, FEI/Philips, USA) at 5 kV accelerating voltage on gold sputter coated samples. Attenuated total reflection-Fourier transform infrared (ATR-FTIR) spectra were measured from 2000 to 500 cm^{-1} at a resolution of 4 cm^{-1} by a Nicolet 6700 spectrometer (Thermo Fisher Scientific, USA). The

measurement of UV absorbance was carried out by using an Evolution 600 UV–vis spectrophotometer (Thermo Fisher Scientific, USA).

Results and discussion

1. Preparation of PVA-*co*-PE nanofibrous membrane

In our previous works, PVA-*co*-PE nanofibers with controlled fiber sizes were successfully fabricated via melt extrusion of immiscible polymer blends of PVA-*co*-PE and CAB. And three-dimensional non-woven like PVA-*co*-PE nanofibrous membranes were prepared via air-spraying coating of well dispersed nanofibers. Their enormous specific surface area and abundant surface hydroxyl groups enable high surface densities of immobilized affinity ligands, further leading to excellent binding capacity of target biomolecules. In addition, unlike poly(vinyl alcohol) (PVA) based membranes that crosslinking treatments are indispensable to provide the stability in aqueous solvent, PVA-*co*-PE membranes do not dissolve in aqueous solution. Moreover, their hydrophilic nature provides the membrane ultra low nonspecific protein adsorption capacity.²⁷⁻²⁹ These merits demonstrate the great potential of PVA-*co*-PE nanofibrous membrane for selective antibody recognition and capture. In this study, an engineered protein ligand, protein A/G, was immobilized onto membrane surfaces to further explore the utilization of PVA-*co*-PE nanofibrous membrane for antibody purification. Figure 1 presents the surface morphologies of the original membrane, the protein ligand attached membrane and the membrane after purification. The uniform nanofiber formation and open porous structure remain intact, indicating the desired mechanical and chemical stability of PVA-*co*-PE nanofibrous membrane during and after ligand attachments and bio-separation processes.

2. Surface activation and protein A/G immobilization

PVA-*co*-PE copolymer with vinyl alcohol content at 73 mol % carries secondary hydroxyl groups at 18.4 mmol/g polymer. The amount of these hydroxyl groups on nanofiber surfaces was determined around 8.9 mmol/g nanofiber in the previous studies.³⁰ Such a high surface density of the reactive sites could contribute to a high amount of immobilized affinity ligands, which subsequently results in a high protein binding capacity. However, these secondary hydroxyl groups cannot be directly used to attach protein ligands. Therefore, as shown in Scheme 1, a variety of activation agents including epibromohydrin (EP), 1,4-butanediol diglycidyl ether (BDGE), oxalyl chloride (OA), nitrophenyl chloroformate (NP), cyanuric chloride (CC), carbonyldiimidazol (CDI), glutaraldehyde (GA) and disuccinimidyl carbonate (DSC) were employed to activate hydroxyl groups on the nanofiber surfaces for subsequent ligand attachment. ATR-FTIR was used to monitor the chemical structure changes after each activation process (Figure 2). For epoxy activations, alkaline condition was used to enhance the nucleophilicity of hydroxyl groups, however, the poor solubilities of EP and BDGE may cause unfavorable contact between material surfaces and chemicals, leading to low reaction yields. Thus, no significant chemical structural change was observed. On the other hand, the strong characteristic peaks of newly formed reactive sites appeared in the spectra after the modification with other six activation methods, and the peaks at 1763 cm⁻¹ (Fig. 2, b), 1761 cm⁻¹ (Fig. 2, c), 1731 cm⁻¹ (Fig. 2, d), 1722 cm⁻¹ (Fig. 2, e), 1756 cm⁻¹ (Fig. 2, f) and 1547 cm⁻¹ (Fig. 2, f) are attributed to the acetyl chloride, nitro phenyl, acyclic carbonate, aldehyde, acyclic carbonate and triazine rings, respectively³⁴⁻³⁶.

The selection of the appropriate reactive sites and coupling reaction pathways is the key factor to determine the amount and accessibility of the protein ligands to be immobilized. In order to screen and determine the optimum activation method, BSA was used as a protein model prior to the protein A/G attachment. BSA is the most common protein used for a broad range of bio-application studies since it is inexpensive and readily available. Herein, the amounts of the immobilized BSA and reaction rates were

investigated (Figure 3). Due to the low coupling yields for epoxy agent, the resulted membranes also exhibit the lowest amount of the immobilized BSA. On the contrary, GA and DSC were found to be the most powerful agents providing the highest BSA coupling amounts after 12 h incubation. In addition, the other four agents presented relatively faster reaction rates thus requiring a shorter incubation time (6 h) to achieve the maximum BSA loading amount. This is probably due to their high reactivity toward the biomolecules. After determining the superiority of GA and DSC activation methods, the membranes modified by these two agents are further used for protein ligand attachment and subsequent antibody purification. By using the bicinchoninic acid based test assay, the amounts of immobilized protein A/G for GA and DSC activation agents were determined at 77.2 and 84.2 mmol/g, respectively. Interestingly, the values of the immobilized protein A/G are lower than the ones of the attached BSA, and this result can be described as the different amounts of lysine residues carried by the protein A/G (36) and BSA (60). As a result, protein A/G possesses less number of primary amine groups from lysine residues to react with the activated membrane surfaces in a comparison to BSA molecule.¹⁰

3. IgG recognition and purification

3.1. Specific recognition of IgG

Protein A/G consists of six binding domains in the form of anti parallel three α -helical bundles, which can independently bind the Fc part of antibodies, such as Immunoglobulin G (IgG). This specific interaction has been widely employed in pharmaceutical applications and biological diagnosis. In this study, the feasibility of selective recognition of IgG molecules by the protein A/G immobilized on PVA-co-PE nanofibrous membranes and their nonspecific protein adsorption were evaluated. And fluorescein isothiocyanate (FITC) labeled human IgG (FITC-IgG) was used for this study since the excited fluorescent dye from IgG can be visualized under fluorescent microscopy and the intensity of the

emitted green signal is proportional to the amount of attached protein molecules. Figure 4 showed the fluorescent microscopy images of original and protein A/G attached GA pre-activated membranes after incubation in FITC-IgG solutions with various concentrations. The light intensities for the ligand attached membranes increased as the increment of antibody concentrations, and the strongest signal at 200 $\mu\text{g/mL}$ indicates a large amount of adsorbed antibody on the membrane surfaces. However, no green signal can be detected for the original membranes under all different conditions. These results demonstrate that the IgG adsorption on the prepared membranes relies on the specific affinity from the immobilized protein A/G. And the original hydrophilic PVA-co-PE nanofibrous membranes exhibits ultralow nonspecific protein adsorption, which is in agreement to the previously reported results.²⁷

3.2. Static IgG binding capacity

The static IgG binding capacities of two protein A/G attached membranes were evaluated via batch wise methods, with one using GA as the activating agent and the other using DSC. It is well known that the parameters on protein adsorption including pH value, ionic strength and initial protein concentration of adsorption media as well as adsorption time play essential roles in impacting static protein binding capacity. In this study, a commercial IgG binding buffer was used due to its optimized conditions of pH and ionic strength. And the effect of the initial protein concentration was studied with IgG concentration ranging from 0.1 to 2.0 mg/mL . As shown in Figure 5, the amounts of adsorbed IgG increase sharply at the beginning and gradually reach the plateau at 1.0 mg/mL . The adsorption times were also determined at 3 h for both two types of affinity membranes to achieve the adsorption saturation. Under this scenario, the static IgG binding capacities of the protein A/G attached membranes with GA and DSC as activation agents were determined at 61.4 and 50.2 mg/g , individually. Meanwhile, the amount of adsorbed IgG on the original membrane was determined as low as 2 mg/mL . It is worth noting that, though GA activated

membranes possess a lower amount of protein ligands with respect to the DSC activated membranes, the former substrate exhibited higher IgG binding capacity. This interesting result can be explained by the spacer effect. Previous study found that, under a high concentration, glutaraldehyde tends to polymerize via acetal reaction mechanism, as illustrated in Scheme 2.^{37, 38} Subsequently, these generated oligomeric long chains on membrane surfaces can act as spacer arms to provide more flexible movement for attached protein ligands and to reduce the steric hindrance from membrane surfaces, facilitating the accessibility of immobilized ligands to target antibodies. In addition, it has been reported that DSC can easily react with hydroxyl and amine groups on protein surfaces in a fast rate which may cause the multi-binding of attached ligands and reduce the ligand's activity by forcing the attached ligand into an unfavorable conformation.³⁹

To further demonstrate these hypotheses, the molar ratio between immobilized protein ligands and adsorbed target antibodies were calculated based on their individual molecular weights. It is clear from Table 1 that 3.8 moles of protein A/G from GA activated membranes are required to bind 1 mole of IgG molecules, while this value increases up to 4.3 moles for DSC activated membranes, indicating that the higher ligand activity from GA chemistry in a comparison to DSC chemistry. Furthermore, each protein A/G contains 6 binding sites for IgG and the molar ratio between the available binding sites and the adsorbed IgG can be also determined. For both affinity membranes, more than 20 moles of binding sites are needed to bind 1 mole IgG, as a result of the high steric hindrance between the binding sites from adjacent ligands. Further increased binding capacity can be achieved by increasing the binding ratio through introducing longer spacers and evenly distributed immobilization.

In order to study the adsorption isotherm of IgG on the prepared nanofibrous membranes, the inverse equilibrium IgG adsorption capacity (q) was plotted against the inverse equilibrium IgG concentration (C), which was illustrated in Figure 6. The resulted linear correlation of these adsorption

data suggests a typical Langmuir adsorption isotherm. Based on the Langmuir equation mentioned above, the maximum IgG binding capacity on the protein A/G attached membranes with GA and DSC as activation agents are calculated as 98.1 and 69.2 mg/g, respectively, which are competent to bead and gel based affinity matrices reported previously.^{40, 41}

3.3. IgG capture from protein mixtures

An ideal affinity membrane for biochromatography should be capable of selectively capturing the protein of interests from a mixture of biomolecules. Afterward, the adsorbed protein can be easily and thoroughly eluted from the solid matrix. To practically evaluate the IgG purification performance, GA activated PVA-co-PE nanofibrous membranes with covalently immobilized protein A/G was immersed in a mixed protein solution in which BSA was added as a model impurity. SDS-PAGE analysis was conducted to identify the protein molecules in original and eluted solutions, and the results are showed in Figure 7. In Lane 2, the top band at 66K Dalton represents the impurity component, BSA. The two bottom bands at 50K and 25K Dalton are attributing to the heavy chain and light chain from IgG molecules, respectively. Originally covalently connected via three pairs of disulfide bonds, the heavy chain and light chain are cleaved after the treatment with loading buffers containing SDS and reducing agent upon heating above 90 °C.⁴² On the other hand, the BSA band completely disappears in Lane c, d and e, which represent the eluted solutions from IgG adsorbed membranes after first, second and third tests. The high purity of the eluted IgG indicates the strong specific affinity between the protein A/G attached membranes and IgG molecules. In addition, the consistent results during three repeating experiments also demonstrate the good stability and reusability of the prepared affinity membranes. To further investigate the desorption efficiency, the IgG concentration in eluted solution is quantified by the

measure of UV absorbance at 280 nm. And the results showed that more than 80% of adsorbed IgG molecules can be eluted and no significant difference of IgG elution rate was found during three trials.

Conclusion

We demonstrated the preparation and application of protein A/G immobilized PVA-*co*-PE nanofibrous membranes for selective antibody recognition and capturing. Prepared by the melt extrusion/air-spraying depositing method, PVA-*co*-PE nanofibrous membranes were treated with versatile surface activating agents to generate the reactive sites for protein ligand immobilization. After screening these surface activations, glutaraldehyde activation method was found as the optimum one to afford a high value of immobilized protein A/G (77.2 mg/g nanofiber), a high ligand activity and excellent IgG binding capacity (61.4 mg/g nanofiber). The ability of selective separation of IgG from protein mixtures by using the prepared affinity membranes was proven by the presence of high purity of IgG from eluted solutions in SDS-PAGE analysis. These results indicated that the protein A/G immobilized GA pre-activated PVA-*co*-PE nanofibrous membranes can serve as a hybrid platform to achieve high selectivity and efficient binding capacity to target antibodies. In addition, the surface chemistry screening study in this work also established empirical guidelines for versatile activation of PVA-*co*-PE polymeric materials and their bio-applications.

Acknowledgements

This research was financially supported by Defense Threat Reduction Agency (HDTRA1-08-1-0005). The author is also grateful to Jastro-Shields Graduate Student Research Fellowship Award at University of California, Davis.

Reference

1. Vijayalakshmi Ayyar, S. Arora, C. Murphy, R. O'Kennedy, *Methods*, 2012, **56**, 116-129.
2. C. Boi, S. Dimartino, C. Sarti, *Biotechnol. Prog.*, 2008, **24**, 640-647.
3. B. Ribeiro, M. Vijayalakshmi Ayyar, D. Todorova-Balvay, A. Bueno, *J. Chromatogr. B*, 2008, **861**, 64-73.
4. S. Hober, K. Nord, M. Linhult, *J. Chromatogr. B*, 2007, **848**, 40-47.
5. G. Fassina, M. Ruvo, G. Palombo, A. Verdoliva, M. Marino, *J. Biochem. Biophys. Methods*, 2001, **49**, 481-490.
6. L. Uzun, D. Türkmen, V. Karakoç, H. Yavuz, A. Denizli, *J. Biomater. Sci.*, 2011, **22**, 2325-2341.
7. C. Boi, *J. Chromatogr. B*, 2007, **848**, 19-27.
8. A. Denizli, *J. Biol. Chem.*, 2011, **39**, 1-18.
9. A. Saxena, P. Tripathi, M. Kumar, K. Shahi, *Adv. Colloid Interface Sci.*, 2009, **145**, 1-22.
10. W. Ma, S. Ramakrishna, *J. Membr. Sci.*, 2008, **319**, 23-28.
11. B. Tennikova, M. Bleha, F. Svec, V. Almazova, G. Belenkii, *J. Chromatogr.*, 1991, **555**, 97-107.
12. L. Hoffer, H. Schwinn, D. Josic, *J. Chromatogr. A*, 1999, **844**, 119-128.
13. D. Josic, A. Buchacher, A. Jungbauer, *J. Chromatogr. B*, 2001, **752**, 191-205.
14. H. Zou, X. Huang, M. Ye, Q. Luo, *J. Chromatogr. A*, 2002, **954**, 5-32.
15. H. Bamford, G. Allamee, *J. Chromatogr.*, 1992, **606**, 19-31.
16. W. Ma, M. Kotaki, S. Ramakrishna, *J. Membr. Sci.*, 2005, **265**, 115-123.
17. J. Kim, E. Hwang, K. Kang, R. Tatavaty, M. Gu, *J. Mater. Chem.*, 2011, **21**, 19203-19206.
18. L. Zhang, T. Menkhaus, H. Fong, *J. Membr. Sci.*, 2008, **319**, 176-184.
19. W. Ma, W. Lan, T. Matsuura, S. Ramakrishna, *J. Chromatogr. B*, 2009, **877**, 3686-3694.

20. T. Zhang, Y. Wei, L. Zhang, B. White, X. Yong, L. Nie, M. Zhu, *J. Mater. Sci.*, 2010, **45**, 2296-2304.
21. T. Menkhaus, H. Varadaraju, L. Zhang, S. Schneiderman, S. Bjustrom, L. Liu, L.; H. Fong, *Chem. Commun.*, 2010, **46**, 3720-3722.
22. C. Tamahkar, C. Babac, T. Kutsal, E. Piskin, A. Denizli, *Process Biochem.*, 2010, **45**, 1713-1719.
23. T. Zhang, L. Nie, G. Yu, Y. Wu, L. Zhang, C. White, M. Zhu, *Desalination*, 2010, **256**, 141-147.
24. F. Che, J. Hou. K. Xu, *J. Membr. Sci.*, 2011, **366**, 272-277.
25. T. Chiu, M. Lin, H. Cheng, Y. Chou, *Polym. Lett.*, 2011, **5**, 308-317.
26. J. Zhu, J. Yang, G. Sun, *J. Membr. Sci.*, 2011, **385-386**, 269-276.
27. J. Zhu, G. Sun, *React. Funct. Polym.*, 2012, **72**, 839-845.
28. J. Zhu, G. Sun, *ACS Appl. Mater. Interfaces*, 2014, **6**, 925-932.
29. J. Zhu, G. Sun, *J. Mater. Chem.*, 2012, **22**, 10581-10588.
30. J. Zhu, G. Sun, *RSC Adv.*, 2014, **4**, 50858-50865.
31. J. Zhu, Q. Bahramian, P. Gibson, H. Schreuder-Gibson, G. Sun, *J. Mater. Chem.*, 2012, **22**, 8532-8540.
32. K. Smith, I. Krohn, T. Hermanson, K. Mallia, H. Gartner, D. Provenzano, K. Fujimoto, M. Goeko, J. Olson, C. Klenk, *Anal. Biochem.*, 1985, **150**, 76-85.
33. P. Dancette, L. Taboureau, E. Tournier, C. Charcosset, P. Blond, *J. Chromatogr. B*, 1999, **723**, 61-68.
34. M. Sánchez-Chaves, C. Ruiz, L. Cerrada, M. Fernández-García, *Polymer*, 2008, **49**, 2801-2807.
35. M. Okubo, Y. Kondo, M. Takahashi, *Polym. Sci.*, 1993, **271**, 109-113.
36. A. Gribov, B. Zubkova, A. Sigarev, *J. Struct. Chem.*, 1993, **34**, 147-154.
37. I. Migneault, C. Dartiguenave, J. Bertrand, C. Waldron, *Biotechniques*, 2004, **37**, 790-802.

38. L. Betancor, F. Lopez-Gallego, A. Hidalgo, N. Alonso-Morales, G. Dellamora-Ortiz, C. Mateo, L. Fernandez-Lafuente, M. Guisan, *Enzym. Microb. Technol.*, 2006, **39**, 877-882.
39. S. Diamanti, S. Arifuzzaman, A. Elsen, J. Genzer, R. Vaia, *Polymer*, 2008, **49**, 3770-3779.
40. H. Alkan, N. Bereli, Z. Baysal, A. Denizli, *Biochem. Eng. J.*, 2009, **45**, 201-208.
41. X. Liu, Y. Guan, Y. Yang, Z. Ma, X. Wu, H. Liu, *J. Appl. Polym. Sci.*, 2004, **94**, 2205-2211.
42. D. Josic, P. Lim, *Technol. Biotechnol.*, 2001, **39**, 215-226.

List of legends

Figure 1. SEM images of (a) original PVA-*co*-PE nanofibrous membrane (b) protein A/G immobilized membrane and (c) membrane after IgG purification

Figure 2. ATR-FTIR analysis of surface activated PVA-*co*-PE nanofibrous membranes: (a) the original membrane, (b) oxalyl chloride, (c) nitrophenyl chloroformate, (d) disuccinimidyl carbonate, (e) glutaraldehyde, (f) carbonyldiimidazol and (g) cyanuric chloride activated membranes.

Figure 3. (a) The amounts of immobilized BSA on various activated PVA-*co*-PE nanofibrous membranes and (b) Reaction rates for BSA immobilization

Figure 4. Fluorescent microscopy images of original and protein A/G immobilized GA pre-activated PVA-*co*-PE nanofibrous membranes after incubating in FITC-IgG solutions with various antibody concentrations

Figure 5. Effect of initial IgG concentration on IgG adsorption on original and protein A/G immobilized PVA-*co*-PE nanofibrous membranes

Figure 6. Linear representation of Langmuir equation of IgG adsorption on protein A/G immobilized PVA-*co*-PE nanofibrous membranes

Figure 7. SDS-PAGE analysis of IgG purifications by protein A/G attached PVA-*co*-PE nanofibrous membranes (Lane a-e represent the biomarker, the protein mixture, the eluted solutions after 1st, 2nd and 3rd trial, individually)

Scheme 1. Surface activations and protein ligand immobilization on PVA-*co*-PE nanofibrous membranes

Scheme 2. GA activated PVA-*co*-PE nanofibrous membranes with long oligomeric chains

Table 1. IgG adsorption on protein A/G immobilized PVA-*co*-PE nanofibrous membranes

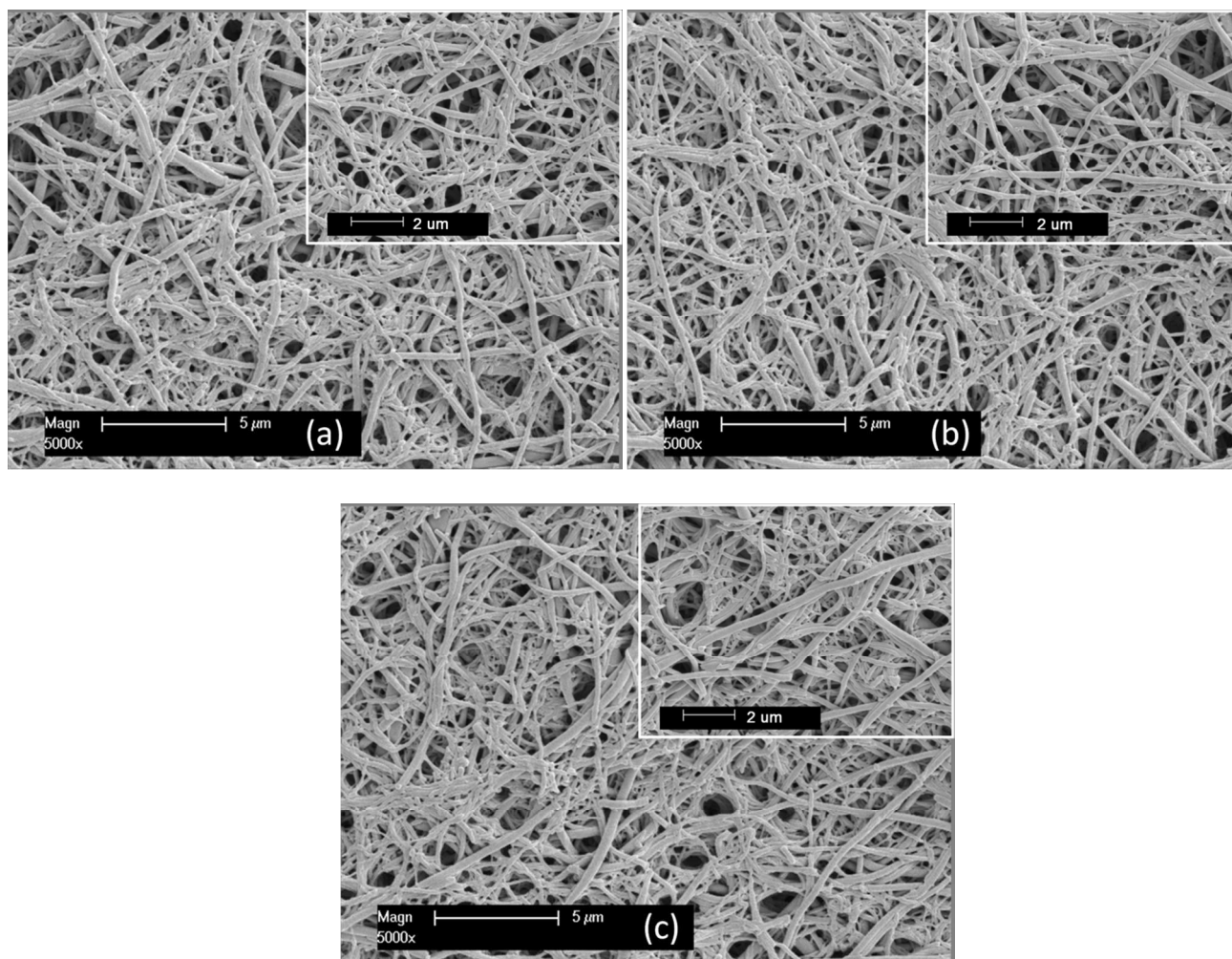


Figure 1. SEM images of (a) original PVA-co-PE nanofibrous membrane (b) protein A/G immobilized membrane and (c) membrane after IgG purification

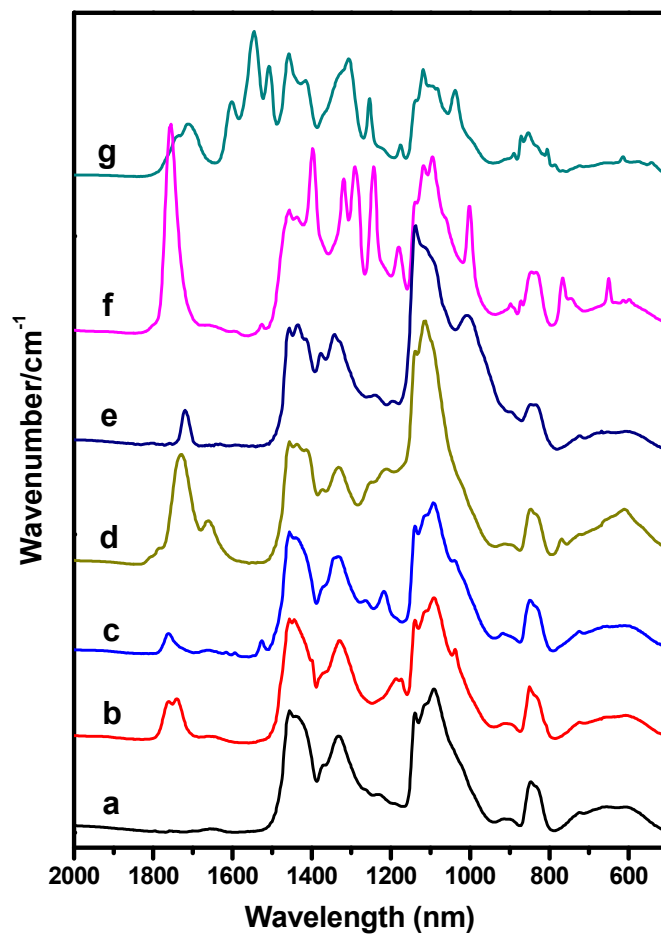


Figure 2. ATR-FTIR analysis of surface activated PVA-co-PE nanofibrous membranes: (a) the original membrane, (b) oxalyl chloride, (c) nitrophenyl chloroformate, (d) disuccinimidyl carbonate, (e) glutaraldehyde, (f) carbonyldiimidazole and (g) cyanuric chloride activated membranes.

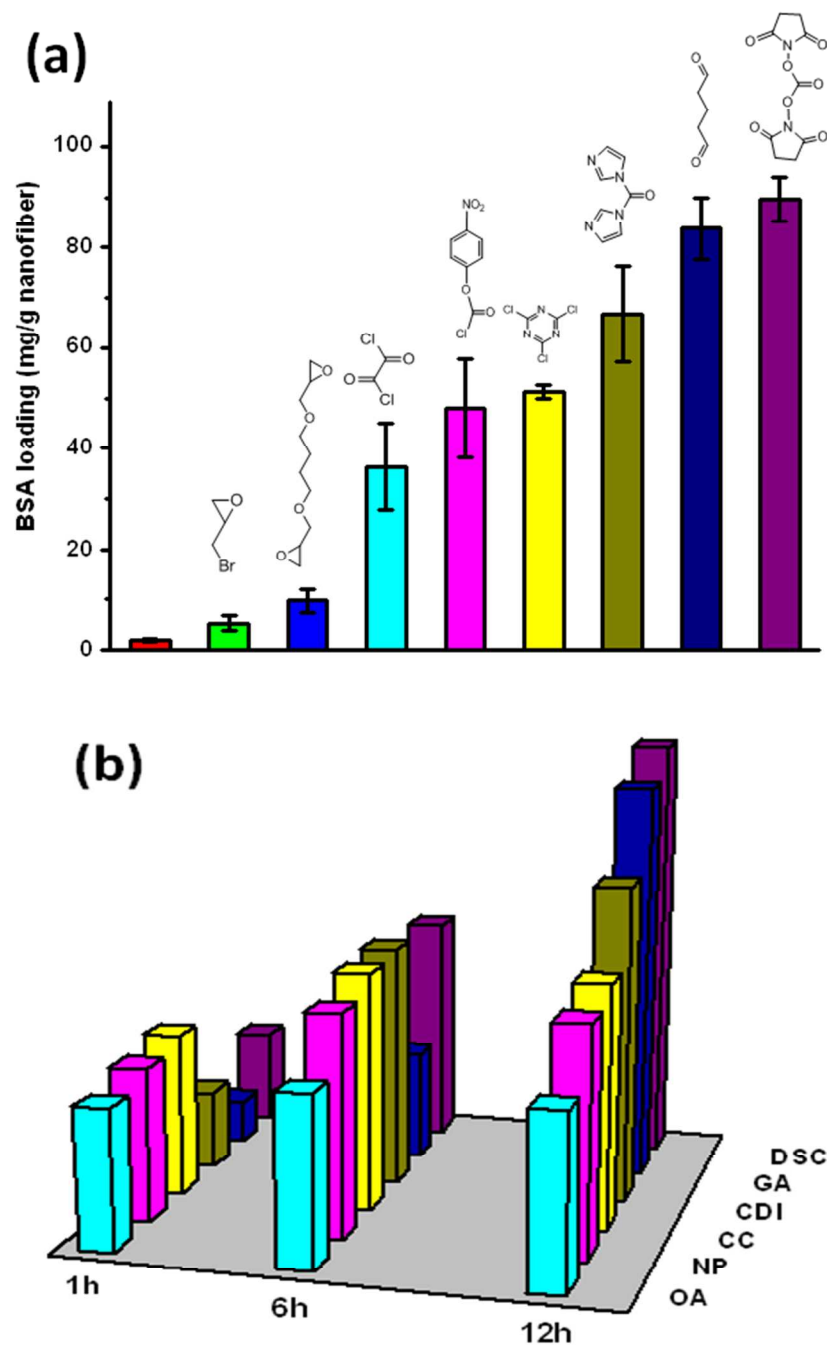


Figure 3. (a) The amounts of immobilized BSA on various activated PVA-co-PE nanofibrous membranes and (b) Reaction rates for BSA immobilization

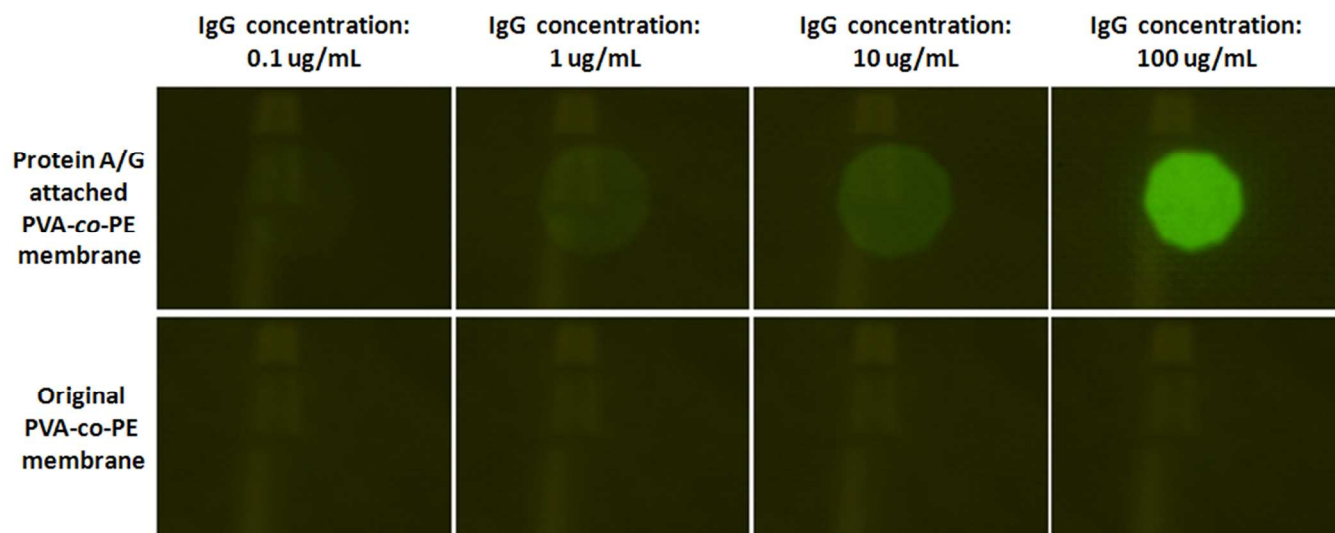


Figure 4. Fluorescent microscopy images of original and protein A/G immobilized GA pre-activated PVA-co-PE nanofibrous membranes after incubating in FITC-IgG solutions with various antibody concentrations

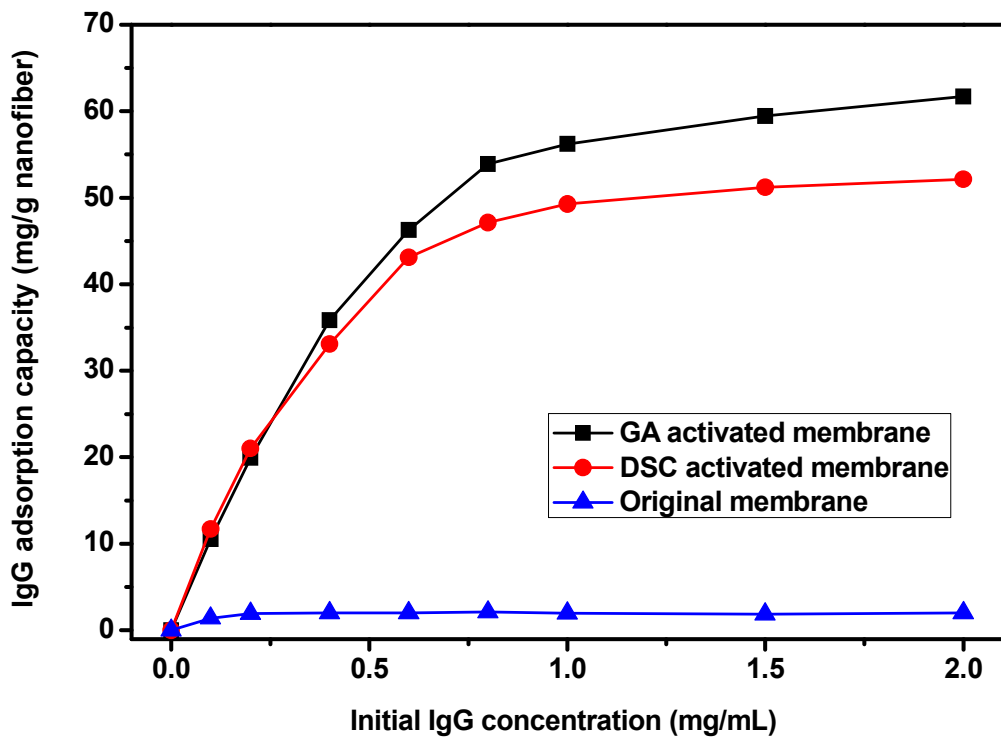


Figure 5. Effect of initial IgG concentration on IgG adsorption on original and protein A/G immobilized PVA-co-PE nanofibrous membranes

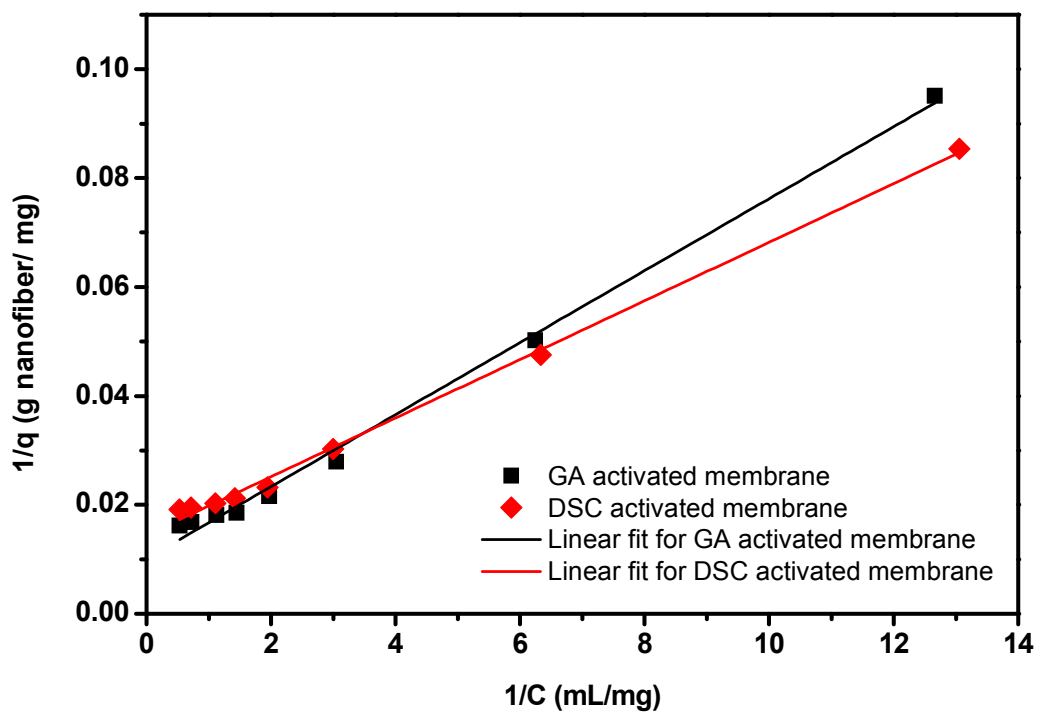


Figure 6. Linear representation of Langmuir equation of IgG adsorption on protein A/G immobilized PVA-co-PE nanofibrous membranes

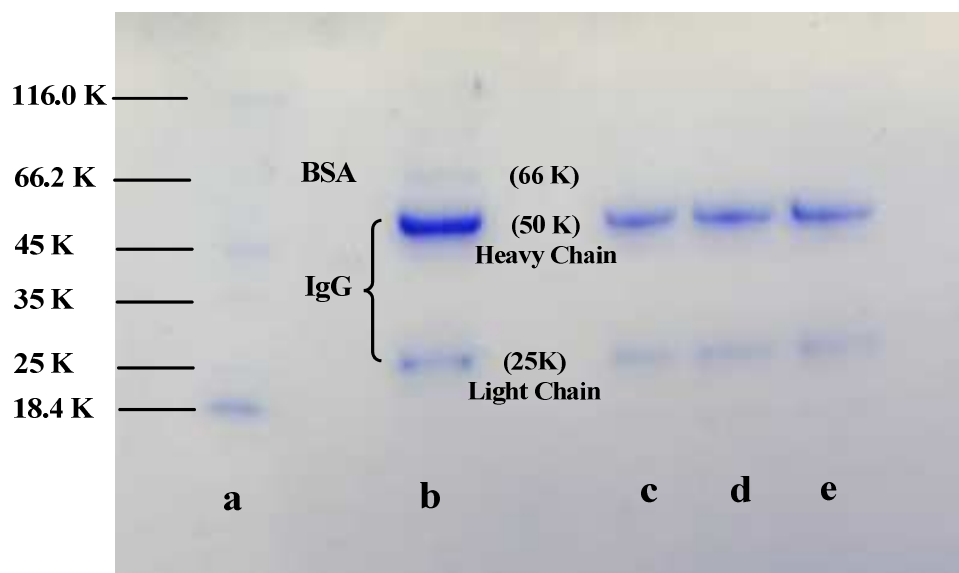
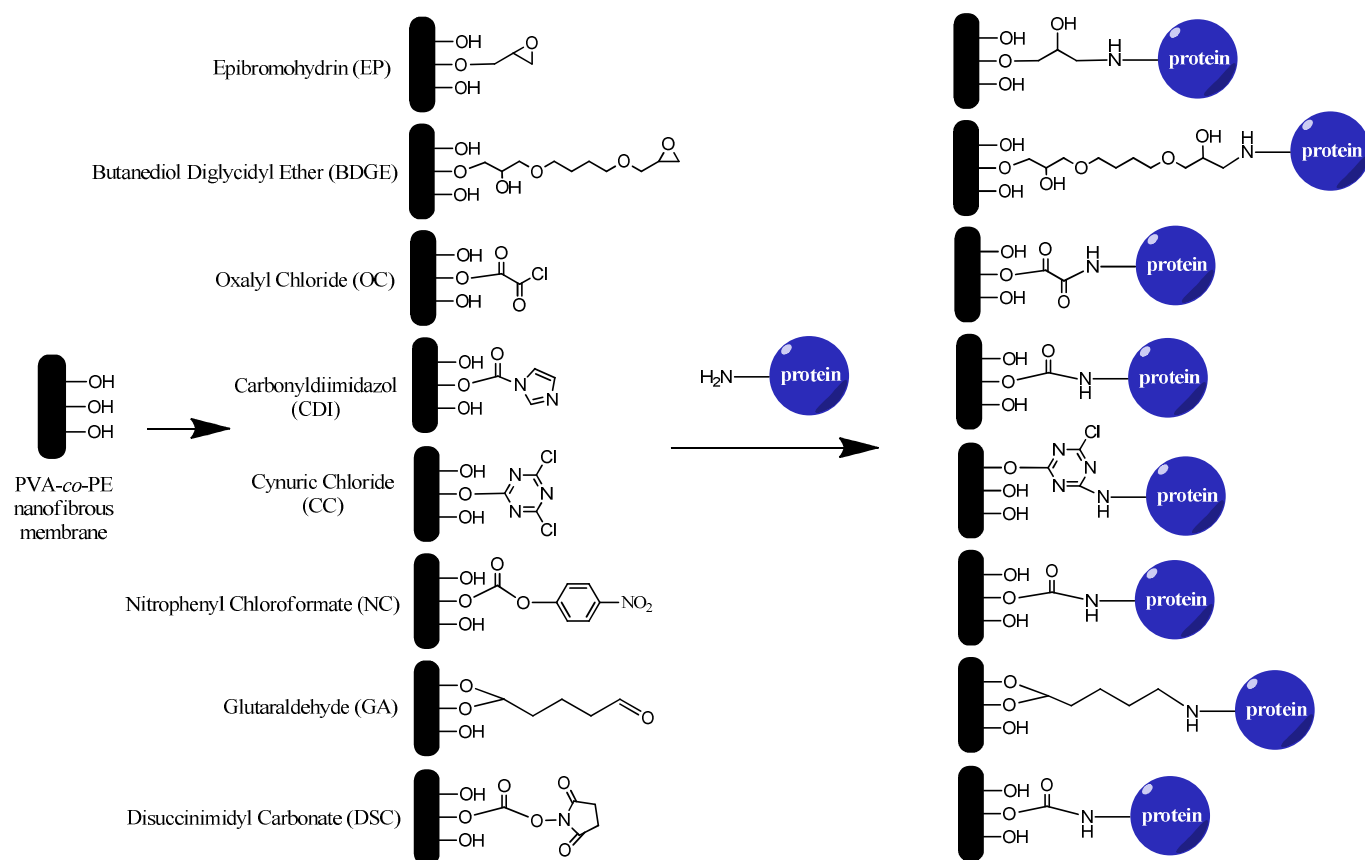
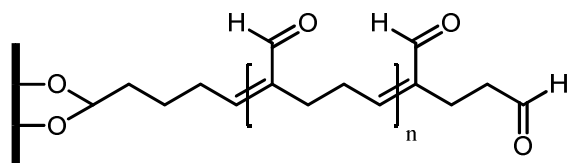


Figure 7. SDS-PAGE analysis of IgG purifications by protein A/G attached PVA-co-PE nanofibrous membranes (Lane a-e represent the biomarker, the protein mixture, the eluted solutions after 1st, 2nd and 3rd trial, individually)



Scheme 1. Surface activations and protein ligand immobilization on PVA-*co*-PE nanofibrous membranes



Scheme 2. GA activated PVA-*co*-PE nanofibrous membranes with long oligomeric chains

Table 1. IgG adsorption on protein A/G immobilized PVA-*co*-PE nanofibrous membranes

Membranes	Protein A/G loading (mg/g)	IgG adsorption capacity (mg/g)	Binding ratio (Ligand/IgG)	Binding ratio (Binding sites/IgG)
GA activated	77.2±4.4	61.4±2.4	3.8	22.7
DSC activated	84.2±2.1	50.2±1.3	5.0	26.1